BJR

https://doi.org/10.1259/bjr.20190710

Received: 14 August 2019 | Revised: 25 May 2020 | Accepted: 09 July 2020

Cite this article as:
Rogers J, Sherwood V, Wayte SC, Duffy JA, Manolopoulos S. Quantification and correction of distortion in diffusion-weighted MRI at 1.5 and 3 T in a muscle-invasive bladder cancer phantom for radiotherapy planning. *Br J Radiol* 2020; **93**: 20190710.

FULL PAPER

Quantification and correction of distortion in diffusion-weighted MRI at 1.5 and 3 T in a muscle-invasive bladder cancer phantom for radiotherapy planning

[1,2]JANE ROGERS, PhD, [2]VICTORIA SHERWOOD, PhD, [2]SARAH C. WAYTE, PhD, [1]JONATHAN A. DUFFY, PhD and [3]SPYROS MANOLOPOULOS, PhD

[1]Department of Physics, University of Warwick CV4 7AL, Warwick, United Kingdom
[2]Clinical Physics and Bioengineering, University Hospitals Coventry and Warwickshire NHS Trust CV2 2DX, Coventry, United Kingdom
[3]Department of Medical Physics and Biomedical Engineering, University College, London WC1E 6BT, United Kingdom

Address correspondence to: Dr Jane Rogers
E-mail: *jane.rogers2@uhcw.nhs.uk*

Objective: Limited visibility of post-resection muscle-invasive bladder cancer (MIBC) on CT hinders radiotherapy dose escalation of the residual tumour. Diffusion-weighted MRI (DW-MRI) visualises areas of high tumour burden and is increasingly used within diagnosis and as a biomarker for cancer. DW-MRI could, therefore, facilitate dose escalation, potentially via dose-painting and/or accommodating response. However, the distortion inherent in DW-MRI could limit geometric accuracy. Therefore, this study aims to quantify DW-MRI distortion via imaging of a bladder phantom.
Methods: A phantom was designed to mimic MIBC and imaged using CT, DW-MRI and T2W-MRI. Fiducial marker locations were compared across modalities and publicly available software was assessed for correction of magnetic susceptibility-related distortion.
Results: Fiducial marker locations on CT and T2W-MRI agreed within 1.2 mm at 3 T and 1.8 mm at 1.5 T. The greatest discrepancy between CT and apparent diffusion coefficient (ADC) maps was 6.3 mm at 3 T, reducing to 1.8 mm when corrected for distortion. At 1.5 T, these values were 3.9 mm and 1.7 mm, respectively.
Conclusions: Geometric distortion in DW-MRI of a model bladder was initially >6 mm at 3 T and >3 mm at 1.5 T; however, established correction methods reduced this to <2 mm in both cases.
Advances in knowledge: A phantom designed to mimic MIBC has been produced and used to show distortion in DW-MRI can be sufficiently mitigated for incorporation into the radiotherapy pathway. Further investigation is therefore warranted to enable individually adaptive image-guided radiotherapy of MIBC based upon DW-MRI.

INTRODUCTION

It has been argued that "the future of image-guided radiotherapy will be MR guided".[1] Indeed, the ultimate goal of MR-guided radiotherapy (MRgRT) is to exploit not only the excellent soft-tissue contrast of MR, but also its ability to use imaging biomarkers and potentially adapt to response during the course of treatment.[1] This use of MR is a form of biology-guided adaptive radiotherapy (BiGART)[2]or theragnostic imaging,[3] which has the potential to be a paradigm shift towards the personalisation of radiotherapy treatment.

Bentzen highlighted theragnostic imaging as the upcoming revolution in radiotherapy,[3] owing to its ability to visualise cellular or biochemical processes by various imaging methods and enable treatments to be individually tailored from this information, minimising damage to nearby healthy tissue. As Fowler noted, the use of ionising radiation for this purpose has the virtue over drug or gene-based therapies that it unambiguously reaches the cells that the physical radiotherapy plan encompasses.[4] In recent years, the interest in incorporating biological information from imaging into radiotherapy treatment has increased.[2,5,6]

One possibility for MRgRT is diffusion-weighted MRI (DW-MRI) and its resulting apparent diffusion coefficient (ADC) maps, which can be used for assessing tumour burden or response to treatment.[7,8] DW-MRI highlights areas of restricted diffusion which occur in regions of increased cellularity such as tumours and has been recommended for testing in clinical trials as a biomarker for cancer.[8] It is used to generate ADC maps, which quantify the degree of reduction in diffusion and have been shown to predict clinical aggressiveness in bladder cancer and hence can be used as a biomarker for this purpose.[9] ADC maps

could therefore potentially enable radiotherapy dose-painting techniques,[3,10,11] allowing treatment to be intensified where the tumour burden is higher. Moreover, changes in ADC values during treatment could be used to assess response and predict efficacy. This would enable individualised adaptations of treatment and hence personalised medicine, whether used within MR-simulation (in place of a planning CT), or via an MR-linac for daily adaptations in treatments.

A potential limitation to the use of DW-MRI is its relatively large inherent geometric distortions compared to CT, which is conventionally used for radiotherapy treatment planning. Thus, it is difficult to accurately infer tumour volumes from DW-MRI, and care must be taken if incorporating positional information from DW-MRI into radiotherapy treatment plans to avoid introducing systematic geometrical errors. A first step in use of DW-MRI for MRgRT is therefore the assessment of the feasibility of using the information DW-MRI conveys to directly influence radiotherapy planning. Later steps will need to include similar assessments for DW-MRI on MR-linacs, as these systems present additional challenges.[12]

Commercial radiotherapy treatment planning systems (TPS) provide methods to geometrically register image datasets to a common coordinate system. Rigid image registration, as used in this study, applies a global transformation for translations and/or rotations of all points in one dataset with respect to the other.[13] This establishes a common coordinate system that is used for subsequent radiotherapy treatment planning. Any remaining spatial errors owing to the imaging methods or registration procedure will propagate through the process and therefore must be understood and accounted for in the design of the treatment plan. IPEM81[14] lists typical radiotherapy systematic geometric uncertainties in the range of 1–3 mm at the 1 s.d. level and recommends tolerances of ±2 mm for most CT-simulator tests. For example, it recommends that the CT-measured distance should agree within ±2 mm with known distances within a phantom. Recommendations for the use of conventional MRI within radiotherapy state that "…it is likely that spatial distortion will be less than 2 mm for images obtained within 15 cm of the isocentre … but this should be verified". Therefore, geometric distortion of DW-MRI below 2 mm would be desirable for incorporation into the radiotherapy pathway.

The BladderPath clinical trial[15] is designed to assess the use of MRI in diagnosis of muscle-invasive bladder cancer (MIBC). As this trial was opening at our centre, this anatomic site was chosen to assess the practicalities involved in further use of such imaging within the radiotherapy pathway for MIBC.

In diagnostic use, DW-MRI is often performed with echo-planar imaging (EPI) sequences; however, EPI techniques are sensitive to magnetic (B_0) field inhomogeneities which result in distortion and signal loss.[16] The American College of Radiology (ACR) MRI phantom[17] is commonly used to assess the magnitude of distortion in MRI using a 2D grid. Figure 1 shows transverse images of an ACR phantom as it appears when imaged using (a) CT, (b) DW-MRI, and (c) following rigid registration of the two. The distortion that can be present in DW-MRI is clearly seen in (b) and (c).

The ACR phantom is not representative of any relevant human anatomy, and its 1-cm-thick grid is of limited use for volumetric evaluation of distortion. Patient images contain temporal variations in bladder filling, so for reproducibility we designed a phantom that emulates MIBC and used it to quantify distortion in DW-MRI via comparison with CT. The magnitude of geometrical distortions present in ADC maps acquired using diagnostic MR scanners were quantified, and the effectiveness of an established method for their correction was assessed. The purpose was to use the MIBC phantom to assess whether DW-MRI data could be incorporated into the radiotherapy treatment planning pathway with acceptable levels of distortion. This paper presents the results of the imaging of this anatomical phantom and interprets them within the context of radiotherapy treatment.

METHODS AND MATERIALS

Phantom design

An internal audit had shown that differences in bladder delineations of up to 8 mm were seen between T2W and ADC maps acquired clinically. It was not possible to determine whether the

Figure 1. Cross-sectional images of ACR MRI phantom using (a) CT, (b) DW-MRI (with b = 300) and (c) following rigid registration of (a) and (b). Imaging parameters used as in Table 2 at 3 T. ACR, American College of Radiology; DW-MRI, diffusion-weighted MRI.

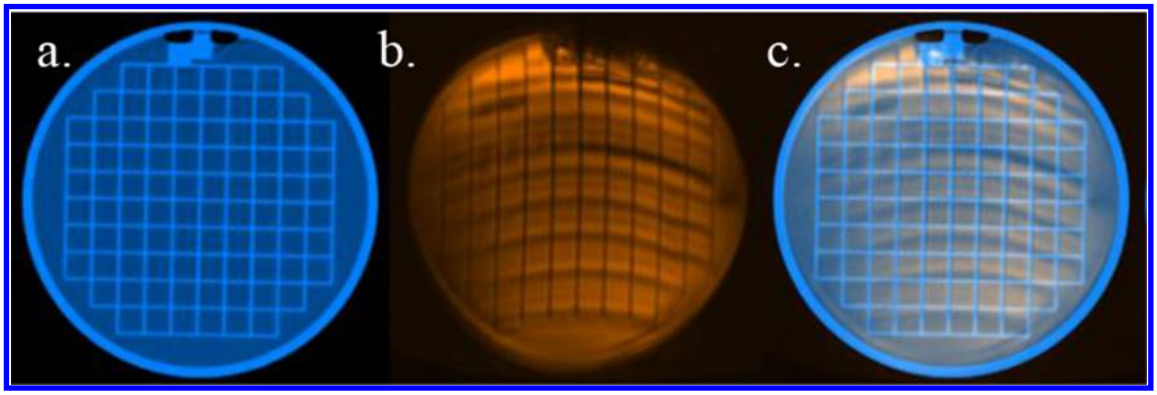

Figure 2. Phantom shown in (a) photograph, (b) diagram of cross-sectional (transverse; TRA) view showing suspension of bladder model, tumour model and string fiducials, (c) orthogonal (sagittal; SAG) view illustrating trapezoidal shape of location aid.

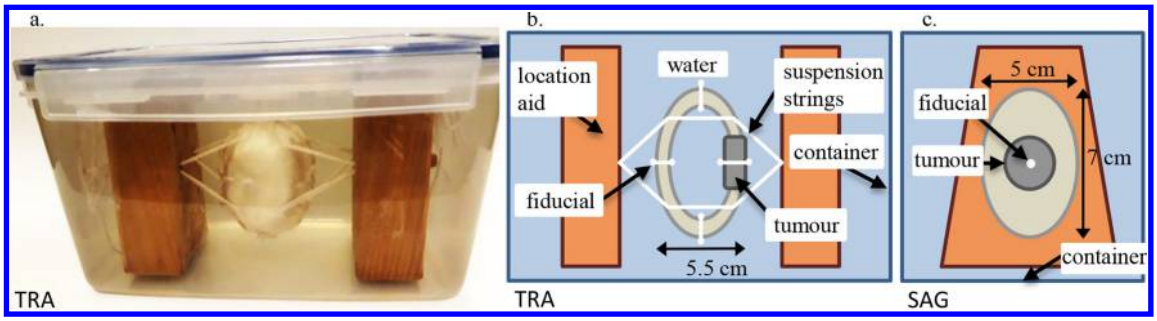

origin of the differences lay in distortions in ADC, changes in bladder and rectal filling between scans, or other sources (*e.g.*, non-axial slicing and rendering variations in display software). A phantom was therefore designed to produce good visibility across the different imaging modalities, utilising fiducial markers to compare locations of points between CT (taken to be the "ground truth") and MRI. The purpose was to assess geometrical uncertainties introduced by the use of DW-MRI without confounding factors of anatomic variations. The following criteria were used in the design of the phantom:

- Constructed using synthetic (non-metallic) components which approximated a urinary bladder containing an internal tumour.
- Produced sufficient contrast across modalities to allow delineation of volumes of interest (clinical image intensities were not intended to be reproduced owing to the technical difficulties in doing so across the three different modalities).
- Contained positional markers for spatial reference.
- Allowed production of artefact-free images.
- Produced extremes of distortion (*e.g.* from air bubbles, with approximately 8 mm considered an upper limit from the internal audit).

This design would therefore produce distortion in keeping with that seen clinically, with susceptibilities similar to those of bladder wall and tumour. It remains technically difficult to produce a phantom which simultaneously reproduces the combinations of electron density and ADC values seen clinically. Therefore, the aim was to produce sufficient contrast for visibility on CT and T2W images, and mean ADC values within 2 s.d. of 1.07 ± 0.27 x 10^{-3} mm^2s^{-1} for the tumour[18] and 1.50 ± 0.71 x 10^{-3} mm^2s^{-1} for the bladder wall.[19] Figure 2(a) shows a photograph of the completed phantom in which the model bladder can be seen suspended between two wooden blocks; these also served as location aids for accurate image registration. Also shown in Figure 2(b) and (c) are orthogonal diagrams in which the internal construction of the bladder wall and tumour is visible along with strings used for suspension of the bladder and fiducial markings.

Table 1. Phantom construction

Item	Material	Size	Comments
Container	Polypropylene	23 × 16 x 13 cm	
Main filling liquid	Undoped water		
Bladder wall	PVA gel	7.0 × 5.5 x 5.0 cm	10% PVA cryogel solution was produced as described in[20] and cast into two moulds with a freeze-thaw cycle repeated three times for adequate rigidity. Thickness 0.5–1.0 cm (also for adequate rigidity).
Tumour	PVA gel, gadolinium (Gd) contrast agent	10 cm^3	10% PVA cryogel solution containing sufficient Gd for good contrast on T2W-MRI was cast into a cylindrical mould and a freeze-thaw cycle repeated five times to produce a degree of contrast with the bladder wall to aid visibility on ADC maps.[21]
Localisation aids	Wood	Upper end 7.0 × 3.8 cm Lower end 9.3 × 3.8 cm	The tapering shape of these wooden blocks enabled accurate rigid registration between CT and MRI
Fiducials	String	0.1 cm diameter	

PVA, polyvinyl alcohol gel; Gd, Gadolinium contrast agent.

Details of materials used and phantom dimensions are listed in Table 1. Features of the phantom construction were:

(1) The main phantom volume was filled with water.
(2) The bladder was cast in two parts using polyvinyl alcohol (PVA) gel, with approximate dimensions taken from the CT of a patient previously treated at our centre; the thickness of the bladder wall was as required for adequate rigidity (0.5–1.0 cm) and therefore greater than that of a patient bladder (typically 0.3 cm). The two parts of the bladder were not sealed and therefore contained water.
(3) The tumour was constructed from PVA gel with a quantity of Gadolinium contrast agent added for good contrast on the T2W images. The volume (10 cm^3) was chosen to be similar to that of a post-resection MIBC tumour as used by Wright et al.[22]
(4) Assembly of the bladder and tumour, and its suspension between the wooden blocks was performed using wet string to minimise introduction of air bubbles as they would cause additional distortion on DW-MRI.
(5) The trapezoidal shape of the wooden blocks enabled accurate rigid registration between image modalities. They also prevented the generation of dielectric artefacts on MRI.
(6) Intersections of string with bladder/tumour surfaces were used as fiducial markers for comparison across the modalities.

Imaging techniques

The phantom was imaged using CT, T2W-MRI and DW-MRI. CT was performed using a GE HiSpeed CT scanner (GE Healthcare, Milwaukee, WI) with the protocol used clinically for pelvic radiotherapy (2.5 mm slice width, 120 kV, 440mA, 1.0 s rotation time, 50.0 cm field of view (FOV)). Multiparametric MRI was performed twice, using a GE 3T Discovery MR750w (GE Healthcare) and a GE 1.5T Optima MR450w scanner (GE Healthcare). All settings used are shown in Table 2 and all images were acquired with automatic shims.

The diffusion sequences used were those in diagnostic clinical use at this site. It is recognised that sequences that will in future be used on an MR-linac will be different, but this work aimed to establish a methodology for quantifying distortion in diffusion sequences and to be relevant for MR radiotherapy-simulation purposes also. The sequences were monopolar, in order to minimise acquisition time. The scanners were operated in research mode for all sequences. Diffusion-weighted images in which the phase encoding blips were positive ("blip-up") as used clinically, and corresponding images with reversed-phase encoding blips ("blip-down") were acquired. The phase-encoding direction was anteroposterior and posteroanterior, respectively. The use of blipped-phase encoding allows incrementation of the position of the k-space trajectory in the phase-encoding direction. The timing of the gradient blips in this direction is such that they coincide with reversal of the readout gradient in the frequency encoding direction. This produces a rectilinear path in k-space, and "blip up" and "blip down" refers to opposing directions of traversal of k-space. In this way, pairs of diffusion-weighted images were acquired with distortions going in opposite directions for each b-value used. ADC map generation was performed automatically using the scanner software to produce ADC "blip-up" and ADC "blip-down" image sets.

Image processing and registration

The CT, T2W-MRI and "blip up" ADC maps were imported directly into RayStation TPS (v.5.0.2.35, RaySearch Laboratories AB, Stockholm, Sweden) from the scanners without further processing. The DICOM "blip-up" and "blip-down" DW-MRIs were converted into NIfTI format using MRIcroGL[23] which was required for processing using the FMRIB Software Library

Table 2. Settings used for T2W and DW-MRI of phantom

Parameters	1.5 T		3.0 T	
	T2w-MRI	*DW-EPI-MRI*	*T2w-MRI*	*DW-EPI-MRI*
TR (ms)	6433	4000	6604	2081
TE (ms)	102.3	70.5	120.3	66
Slice thickness (mm)	2.5	2.5	2.5	2.5
Slice gap (mm)	0	0	0	0
No. of slices	36	36	36	36
Matrix size	256 × 224	140 × 70	352 × 288	140 × 70
FOV (cm)	24 × 24	24 × 24	24 × 24	24 × 24
Echo train length	21	-	19	-
Acquisition time (min)	6:00	3:36	5:24	2:30
b-values	-	0, 50, 300, 700, 1000	-	0, 50, 300, 700, 1000
NEX	-	1	-	1
Pixel bandwidth (Hz)	244.141	1953.12	139.492	1953.12

EPI, echo-planar imaging; T2w-MRI, T_2-weighted MRI; DW-MRI, diffusion-weighted MRI; TR, time of repetition; TE, echo time; FOV, field of view; NEX, number of excitations.

Figure 3. Cross-sectional images of the phantom on (a) CT, (b) T2W-MRI, (c) registration of CT and T2W-MRI, (d) ADC "blip-up", (e) ADC "blip-down", (f) ADC "corrected", (g) registration of CT and ADC "blip-up", (h) registration of CT and ADC "blip-down", (i) registration of CT and ADC "corrected". "Blip-up" and "blip-down" refer to k-space readout direction; ADC "corrected" map was recalculated following distortion-correction of acquired DW-MRIs using FSL. All MR images shown here were acquired using a 3 T scanner. Scaling is the same for all images, as indicated by inset in (c).

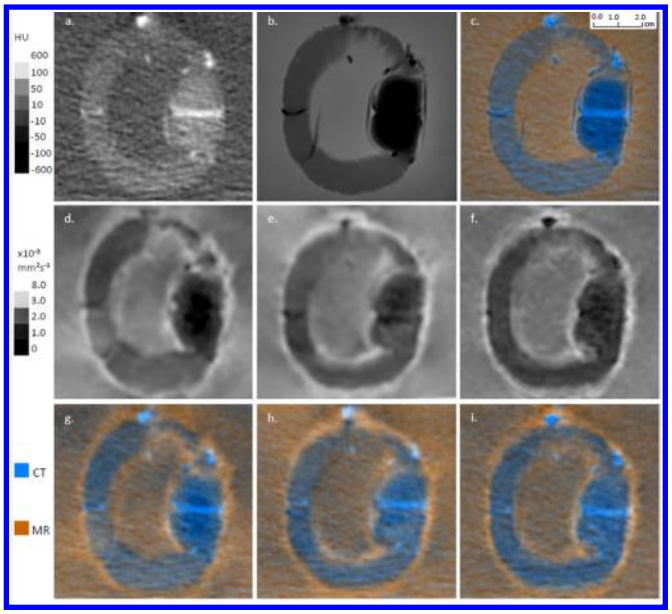

(FSL), (FMRIB Analysis Group, Oxford, UK). From the paired images (blip-up and blip-down), the susceptibility-induced off-resonance field was estimated using a method similar to that described by Andersson et al.,[24] as implemented in FSL[25] and the two images were combined into a single distortion-corrected one for each b-value used. The corrected images were imported into MATLAB (MATLAB R2018a, MathWorks, Natick, MA) and a new ADC map created (ADC "corrected") and converted into DICOM format. These corrected ADC maps were then imported into RayStation TPS.

The bladder outer surface, tumour, location aids and string were delineated on all imported image sets. Fiducial marker locations were assigned points of interest (POIs) at the intersection of string with relevant bladder wall or tumour surface.

Rigid registration of the T2W-MRI to CT was performed manually using the location aids to position accurately in three orthogonal directions and with respect to three axes of rotation. This transformation was then applied to both ADC maps ("blip-up" and "corrected") resulting in the same rigid registration of each ADC map to CT.

RESULTS

Representative images of the phantom are shown in Figure 3, with (a) CT, (b) T2W-MRI, (c) registration of CT and T2W-MRI, (d)-(f) ADC maps and (g)-(i) registrations of CT and ADC maps. These images show that the distortions are displaced in opposite directions between the "blip-up" and "blip-down" ADC maps, with the bladder appearing shorter in the vertical direction in the "blip-down" image than in the "blip-up" image. The corrected ADC shows visibly reduced distortion. The mean ± 1 s.d. ADC values in the "blip up" images were 1.58 ± 0.08 x 10^{-3} mm^2s^{-1} and 1.88 ± 0.05x 10^{-3} mm^2s^{-1} in the tumour and bladder wall, respectively, at 3 T, and 1.59 ± 0.12 x 10^{-3} mm^2s^{-1} and 1.80 ± 0.03x 10^{-3} mm^2s^{-1} at 1.5 T. The stated aim was to produce a phantom with mean ADC values within 2 s.d. of 1.07 ± 0.27 x 10^{-3} mm^2s^{-1} for the tumour[18] and 1.50 ± 0.71x 10^{-3} mm^2s^{-1} for the bladder wall.[19] Hence, the phantom has met this aim (within 1 s.d. for the bladder wall and 2 s.d. for the tumour).

Quantitative analysis was performed between the CT (taken as "ground truth") and ADC maps acquired using the clinical setting of the MR scanners (*i.e.*, "blip-up"). This was compared with the same analysis for the corrected ADC maps (the "blip-down" DW-MRIs were used only for correction of distortions within FSL).

The distance to agreement for each POI (fiducial) was generated automatically by the TPS via the image registration module. Figure 4 shows the mean distances to agreement of 14 POIs on T2W-MRI, ADC "blip-up", and ADC "corrected" compared to their locations on CT. The components in each of the left-right, superior-inferior and anteroposterior directions are shown as well as the total distance. In this way, the positional information from CT was taken to be the "ground truth", with the magnitude of the effects of distortion then compared between T2W-MRI (with minimal expected geometric distortion) and the two ADC maps. The dashed lines at 2 mm indicate the maximum tolerance usually accepted clinically for anatomic MRIs within radiotherapy.[14]

For T2W-MRI at 3 T, the mean (and maximum) discrepancy in POI location compared to CT was 0.8 ± 0.2 mm (1.2 mm at maximum). At 1.5 T, these results are 1.1 ± 0.4 mm (1.8 mm maximum). The equivalent results for "blip-up" ADC maps showed a mean location discrepancy of 2.2 ± 1.7 mm (6.3 mm maximum) at 3 T and 2.3 ± 1.1 mm (3.9 mm maximum) at 1.5 T. The corresponding ADC "corrected" values were 1.3 ± 0.3 mm (1.8 mm maximum) at 3 T and 1.1 ± 0.4 mm (1.7 mm maximum) at 1.5 T, respectively. At both 3 T and 1.5 T, the worst agreement between ADC "blip up" and CT occurs in the anteroposterior direction, which was the phase-encoding direction for MR acquisitions. The agreement is improved in both cases by the use of the FSL to produce ADC corrected.

Figure 5 shows the distance to agreement for the POIs with distance from isocentre. Where the superior-inferior distances were the same, the mean distance to agreement is shown for clarity. The greatest distance to agreement is at the furthest superior and inferior extents, particularly at 3 T. The trend is no longer visible after distortion correction.

DISCUSSION

Various techniques exist to minimise or counter the effects of geometric distortion in DW-MRI; however, the requirements

Figure 4. Box and whisker plot showing distances to agreement for (a) 3 T and (b) 1.5 T scanners, respectively, in the left-right (L/R), superior-inferior (S/I) and anteroposterior (A/P) directions and in total (*i.e.,* the sum in quadrature). Orientation in scanners is head-first supine. Marker locations shown relative to CT for T2W-MRI, ADC "blip-up" and ADC corrected with dashed line indicating maximum acceptable for radiotherapy purposes.[14] (Boxes show median and interquartile range, whiskers indicate minimum and maximum values.)

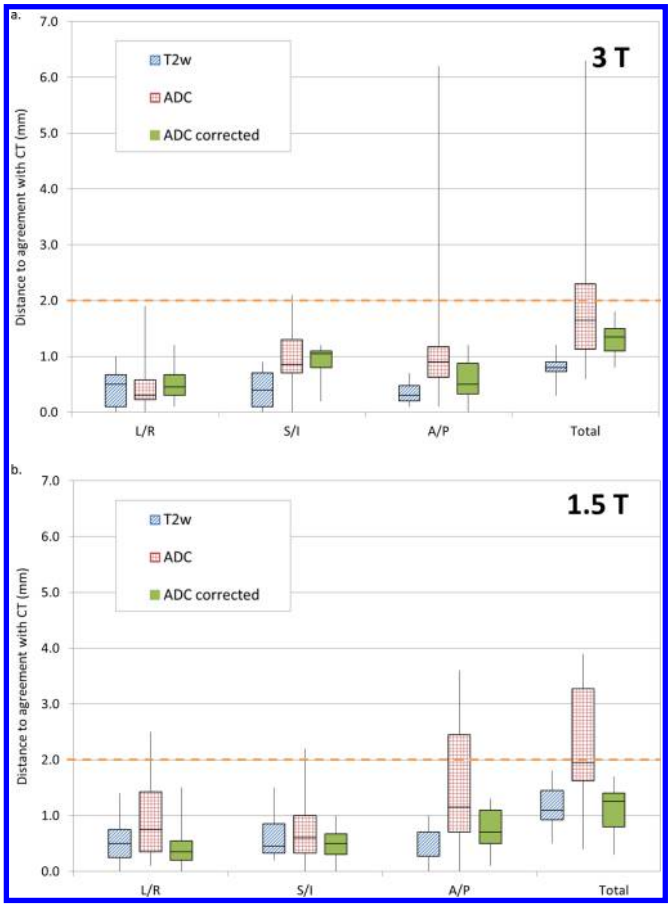

Figure 5. Distances to agreement for (a) 3 T and (b) 1.5 T scanners, respectively, with POI location relative to isocentre in the superior-inferior direction. Marker locations shown relative to CT for T2W, ADC "blip-up" and ADC corrected, with error bars showing estimated errors and with dashed line indicating maximum acceptable for radiotherapy purposes.[14]

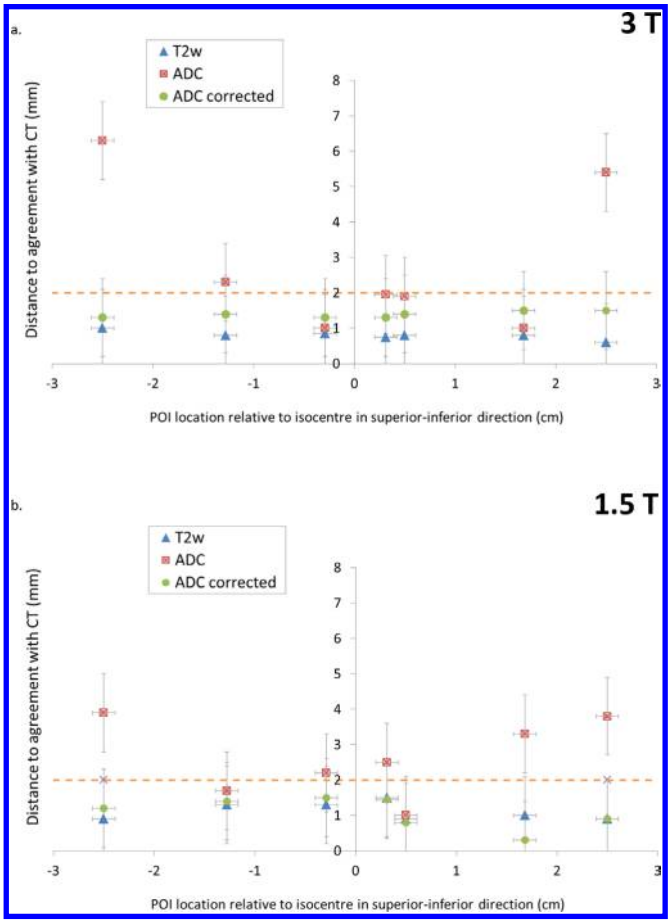

of image fidelity and workflows within a diagnostic context are different to those within radiotherapy treatment planning. The purpose of this work was not to examine or compare methods of image distortion correction but to assess in the context of radiotherapy treatment whether one particular existing method (*i.e.,* the use of FSL software) is sufficient to enable the use of DW-MRI for determining the target volume. Further work will be required to assess the potential impact that this approach to the radiotherapy treatment process might have (including assessment of signal change effects on dose-painting techniques). As a consequence, only one widely used method for distortion-correction of EPI-based DW-MRI is tested here, although future work using different DWI sequences could further reduce distortion (*e.g.,* TSE readout-based sequences.[26,27]

Our data showed that for T2W-MRI at 3 T the discrepancy in POI location was 0.8 mm on average, and 1.2 mm at maximum. Similarly, at 1.5 T, these results are 1.1 mm (mean) and 1.8 mm (maximum), respectively. However, the equivalent results for "blip-up" ADC maps showed that while the mean location discrepancy was 2.2 mm, the maximum exceeded 6 mm at 3 T. At 1.5 T, the corresponding results were 2.3 mm (mean) and 3.9 mm (maximum). These results show that while the T2W images are within the IPEM81 recommendations for radiotherapy images, those for the ADC maps acquired at both 3 T and 1.5 T are greater than the desirable 2 mm tolerance.[14] Therefore, at both 3 T and 1.5T, the distortion seen in ADC maps acquired using current clinical protocols with no further processing would be unacceptable for the purposes of target delineation and subsequent dose escalation in radiotherapy.

The fiducials which showed the poorest agreement were located at the furthest superior and inferior extremes of the bladder for images acquired using both scanners. A possible reason for this could be that the centre of the scanned volume is positioned at the centre of the bore longitudinally, and therefore any field inhomogeneities would be worse for slices further from the centre of the phantom. The discrepancies occurred predominantly in the phase-encoding direction and the effect was more pronounced for the 3 T images, as would be expected.

Following distortion-correction of the DW-MRIs using FSL, and subsequent recalculation of ADC maps, the mean (and maximum) discrepancies in fiducial locations were 1.3 mm (1.8 mm) at 3 T and 1.1 mm (1.7 mm) at 1.5 T, respectively. These results were similar to the T2W images, and <2 mm in all directions. Therefore, using this method to correct the distortion of DW-MRI and ADC maps for radiotherapy, delineation and dose escalation purposes appear feasible, and further work to assess this process in patient images is therefore worthwhile. The next steps should include assessments of effects of nearby air pockets on distortions, as these could be significant in the pelvis.

The phantom design using string fiducials is limited in its ability to detect residual distortion below approximately 1 mm, as this is similar to the thickness of the string. Should additional measurements be required to assess further reduction in distortion, revision of the phantom design and imaging parameters to detect these differences would be required. The work undertaken here corrected only for magnetic susceptibility-related distortions, and it is appreciated that a further reduction in distortion could be achieved via use of eddy current-related corrections. Similarly, as the MRI sequences used for this work used monopolar encoding gradients to minimise scanning time, future work could investigate whether bipolar sequences would further reduce distortions. However, such sequences may take longer and therefore could lead to increased likelihood of patient movement and issues with increased bladder filling over the course of imaging. These issues would be particularly important should this technique be used on an MR-linac prior to radiotherapy delivery.

An initial approach to the use of this additional imaging information for the purposes of radiotherapy could be via a simultaneous integrated boost (SIB), in which results such as those discussed in this paper inform the magnitude of the margin for the boost volume. At present, the ADC values and corresponding appropriate boost doses are not yet known; for such clinical trials to be undertaken, the first steps will include work such as that described here. Ultimately, it could be expected that an online-adaptive individualised approach to treatment adaptation would be taken, in which changes in ADC would inform treatment adaptation. However, there would first need to be further work to enable a streamlined workflow incorporating the image distortion corrections. At present, this is only feasible offline and in a research environment. This work provides a proof of principle, with the aim that functionality to enable the required workflow would be forthcoming in the future. The differences in design of MR-linacs compared to diagnostic MR scanners[12] would require this approach or similar to also be performed for validation.

CONCLUSION

A phantom was designed to determine the effect of distortions in ADC maps on positional information in MIBC. ADC maps computed by the scanner from "blip-up" DW-MRI and transferred to a CT frame-of-reference reproduced location within 6.3 mm at 3 T and 3.9 mm at 1.5 T. However, when the DW-MRIs were corrected for distortion, fiducial locations were reproduced within 1.8 mm for both scanners. This was similar to the reproducibility of fiducial location found between CT and T2W-MRI and is less than the 2 mm tolerance frequently used for application of standard MR into radiotherapy planning.

This work indicates that MRgRT using DW-MRI is possible for MIBC based on the phantom results, and that further work to assess its use with clinical images is required. This approach to radiotherapy treatment could result in a major shift towards biological-adaptation of radiotherapy treatments from the current position of being guided purely by anatomic imaging.

Our work in quantifying the magnitude of geometrical distortion for a particular anatomical site and imaging modality highlights the need for further work to determine similar information for other sites and modalities where imaging will be used for biologically adaptive radiotherapy treatments. In addition, it is necessary to investigate further the dosimetric impact and clinical effect on tumour control which would be expected by such biologically adapted radiotherapy treatments.

ACKNOWLEDGMENT

The authors would like to thank Pete Mulholland and Ryan Gilder for their construction of the phantom, RaySearch Laboratories for their help in answering our queries, and Prof Nicholas James for useful conversations and background clinical information about MIBC. We also wish to thank GE Healthcare for our MR research agreement and in particular Gavin Houston for his help and advice in acquiring the EPI data.

REFERENCES

1. Pollard JM, Wen Z, Sadagopan R, Wang J, Ibbott GS. The future of image-guided radiotherapy will be MR guided," *British Journal of Radiology*. 2017; **90**, , (no. 1073)vol..
2. Grau C, Høyer M, Alber M, Overgaard J, Lindegaard JC, Muren LP. Biology-guided adaptive radiotherapy (BiGART)--more than a vision? *Acta Oncol* 2013; **52**, , (no. 7): 1243–7. doi: https://doi.org/10.3109/0284186X.2013.829245
3. Bentzen SM. Theragnostic imaging for radiation oncology: dose-painting by numbers. *Lancet Oncol* 2005; **6**: 112–7. doi: https://doi.org/10.1016/S1470-2045(05)01737-7
4. Fowler JF. Development of radiobiology for oncology-a personal view. *Phys Med Biol* 2006; **51**: R263–86. doi: https://doi.org/10.1088/0031-9155/51/13/R16
5. Grau C, Høyer M, Poulsen PR, Muren LP, Korreman SS, Tanderup K, et al. Rethink radiotherapy - BIGART 2017. *Acta Oncol*, 2017; . **56**: 1341–52. doi: https://doi.org/10.1080/0284186X.2017.1371326
6. Grau C, Overgaard J, Høyer M, Tanderup K, Lindegaard JC, Muren LP. Biology-guided adaptive radiotherapy (BiGART) is progressing towards clinical reality. *Acta Oncol*, 2015; . **54**: 1245–50. doi: https://doi.org/10.3109/0284186X.2015.1076992
7. Malayeri AA, El Khouli RH, Zaheer A, Jacobs MA, Corona-Villalobos CP, Kamel

IR, et al. Principles and applications of diffusion-weighted imaging in cancer detection, staging, and treatment follow-up. *Radiographics* 2011; **31**, , (no. 6): 1773–91. doi: https://doi.org/10.1148/rg.316115515

8. Padhani AR, Liu G, Koh DM, Chenevert TL, Thoeny HC, Takahara T, et al. Diffusion-Weighted magnetic resonance imaging as a cancer biomarker: consensus and recommendations. *Neoplasia* 2009; **11**, , (no. 2): 102–25. doi: https://doi.org/10.1593/neo.81328
9. Kobayashi S, Koga F, Yoshida S, Masuda H, Ishii C, Tanaka H, et al. Diagnostic performance of diffusion-weighted magnetic resonance imaging in bladder cancer: potential utility of apparent diffusion coefficient values as a biomarker to predict clinical aggressiveness. *Eur Radiol* 2011; **21**, , (no. 10): 2178–86. doi: https://doi.org/10.1007/s00330-011-2174-7
10. Ling CC, Humm J, Larson S, Amols H, Fuks Z, Leibel S, et al. Towards multidimensional radiotherapy (MD-CRT): biological imaging and biological conformality. *Int J Radiat Oncol Biol Phys* 2000; **47**, , (no. 3): 551–60. doi: https://doi.org/10.1016/S0360-3016(00)00467-3
11. Hall EJ. Dose-painting by numbers: a feasible approach? *Lancet Oncol* 2005; **6**, , (no. 2), : 66vol.p.. doi: https://doi.org/10.1016/S1470-2045(05)01718-3
12. Datta A, Aznar MC, Dubec M, Parker GJM, O'Connor JPB. Delivering functional imaging on the MRI-Linac: current challenges and potential solutions. *Clin Oncol*, 2018; **30**: 702–10. doi: https://doi.org/10.1016/j.clon.2018.08.005
13. Kessler ML. Image registration and data fusion in radiation therapy. *Br J Radiol* 2006; **79 Spec No 1**: 99–108pp.. doi: https://doi.org/10.1259/bjr/70617164
14. Patel I, Weston S, Palmer AL, Mayles WPM, Whittard P, Clements Ret al. Physics Aspects of Quality Control in Radiotherapy.. In: ed.,*IPEM Report 81., 2*. York: Institute of Physics and Engineering in Medicine; 2018.
15. James N. Bladderpath clinical trial. December 2019URL. Available from: https://www.birmingham.ac.uk/research/activity/mds/trials/crctu/trials/Bladder-Path/investigators.aspx.
16. Farzaneh F, Riederer SJ, Pelc NJ. Analysis of T2 limitations and off-resonance effects on spatial resolution and artifacts in echo-planar imaging. *Magn Reson Med* 1990; **14**, , (no. 1): 123–39. doi: https://doi.org/10.1002/mrm.1910140112
17. ACR. [Online].Available from: https://www.acraccreditation.org//media/ACRAccreditation/Documents/MRI/LargePhantomGuidance.pdf?la=en..
18. Takeuchi M, Sasaki S, Ito M, Okada S, Takahashi S, Kawai T, et al. Urinary bladder cancer: diffusion-weighted MR imaging--accuracy for diagnosing T stage and estimating histologic grade. *Radiology* 2009; **251**(no. 1): 112–21. doi: https://doi.org/10.1148/radiol.2511080873
19. El-Assmy A, Abou-El-Ghar ME, Refaie HF, Mosbah A, El-Diasty T. Diffusion-Weighted magnetic resonance imaging in follow-up of superficial urinary bladder carcinoma after transurethral resection: initial experience. *BJU Int* 2012; **110**(11 Pt B): E622–7. doi: https://doi.org/10.1111/j.1464-410X.2012.11345.x
20. Mano I, Goshima H, Nambu M, Iio M. New polyvinyl alcohol gel material for MRI phantoms. *Magn Reson Med* 1986; **3**: 921–6. doi: https://doi.org/10.1002/mrm.1910030612
21. Dwihapsari Y, Sari DP. The assessment of consistency using penetrometer and apparent diffusion coefficient (ADC) value using diffusion weighted magnetic resonance imaging (DW-MRI) from polyvinyl alcohol formed by freezing-thawing cycle. *AIP Conference Proceedings* 2012; **1454**: 53–6.
22. Wright P, Muren LP, Høyer M, Malinen E. Evaluation of adaptive radiotherapy of bladder cancer by image-based tumour control probability modelling. *Acta Oncol* 2010; **49**(no. 7): 1045–51. doi: https://doi.org/10.3109/0284186X.2010.498431
23. Rorden C, Brett M. Stereotaxic display of brain lesions. *Behav Neurol* 2000; **12**, , (no. 4): 191–200. doi: https://doi.org/10.1155/2000/421719
24. Andersson JLR, Skare S, Ashburner J. How to correct susceptibility distortions in spin-echo echo-planar images: application to diffusion tensor imaging. *Neuroimage* 2003; **20**(no. 2): 870–88. doi: https://doi.org/10.1016/S1053-8119(03)00336-7
25. Smith SM, Jenkinson M, Woolrich MW, Beckmann CF, Behrens TEJ, Johansen-Berg H, et al. Advances in functional and structural Mr image analysis and implementation as fsl. *Neuroimage* 2004; **23 Suppl 1**: S208–19. doi: https://doi.org/10.1016/j.neuroimage.2004.07.051
26. Panyarak W, Chikui T, Yamashita Y, Kamitani T, Yoshiura K. Image quality and ADC assessment in turbo spin-echo and Echo-Planar diffusion-weighted MR imaging of tumors of the head and neck. *Acad Radiol* 2019; **26**: e305-–16. doi: https://doi.org/10.1016/j.acra.2018.11.016
27. Hirata K, Nakaura T, Okuaki T, Kidoh M, Oda S, Utsunomiya D, et al. Comparison of the image quality of Turbo spin echo- and echo-planar diffusion-weighted images of the oral cavity. *Medicine* 2018; **97**: e0447. doi: https://doi.org/10.1097/MD.0000000000010447